Biomed Microdevices (2014) 16:537–548
DOI 10.1007/s10544-014-9856-2

Microfluidic platform for negative enrichment of circulating tumor cells

Bhuvanendran Nair Gourikutty Sajay · Chia-Pin Chang · Hamizah Ahmad · Puttachat Khuntontong · Chee Chung Wong · Zhiping Wang · Poenar Daniel Puiu · Ross Soo · Abdur Rub Abdur Rahman

Published online: 27 March 2014

Abstract Negative enrichment is the preferred approach for tumor cell isolation as it does not rely on biomarker expression. However, size-based negative enrichment methods suffer from well-known recovery/purity trade-off. Non-size based methods have a number of processing steps that lead to compounded cell loss due to extensive sample processing and handling which result in a low recovery efficiency. We present a method that performs negative enrichment in two steps from 2 ml of whole blood in a total assay processing time of 60 min. This negative enrichment method employs upstream immunomagnetic depletion to deplete CD45-positive WBCs followed by a microfabricated filter membrane to perform chemical-free RBC depletion and target cells isolation. Experiments of spiking two cell lines, MCF-7 and NCI-H1975, in the whole blood show an average of >90 % cell recovery over a range of spiked cell numbers. We also successfully recovered circulating tumor cells from 15 cancer patient samples.

Keywords Circulating tumor cells (CTCs) · Cancer cell isolation · Metastasis · Negative enrichment · White blood cell (WBC) depletion

Abbreviation

CTC	Circulating tumor cells
WBC	White blood cell
RBC	Red blood cell
EMT	Epithelial to mesenchymal transition
TAC	Tetrameric antibody complexes
GFP	Green florescent protein
PBS	Phosphate buffered saline
EpCAM	Epithelial cell adhesion molecule

1 Introduction

The significance of CTCs for clinical cancer management has been widely recognized (Rolle et al. 2005; Zieglschmid et al. 2005; Kahn et al. 2004; Racila et al. 1998). Despite many efforts to develop technologies for tumor cell isolation, it has been noted that an optimal technology is still unavailable. Our current understanding of clinical significance of CTCs is biased on the technology used (Riethdorf and Pantel 2008; Budd 2009). Without an unbiased, standardized and optimized method for CTC isolation, CTCs may generate poor clinical interest. Many novel technologies have demonstrated significantly better performance than FDA-approved CellSearch® platform, which is currently used in most clinical trials to establish the utility of CTCs for clinical cancer management (Marrinucci et al. 2010; Desitter et al. 2011; Lim

Bhuvanendran Nair Gourikutty Sajay and Chia-Pin Chang contributed equally to this paper.

B. N. G. Sajay · C.-P. Chang (✉) · H. Ahmad · C. C. Wong · A. R. A. Rahman
BioElectronics Programme, Institute of Microelectronics, A*STAR (Agency for Science, Technology and Research), 1 Science Park Road, Singapore 117528, Singapore
e-mail: changcp@ime.a-star.edu.sg

B. N. G. Sajay · P. D. Puiu
NOVITAS- Nanoelectronics Centre Of Excellence, School of Electrical and Electronics Engineering, Nanyang Technological University, 50 Nanyang Avenue, Singapore 639798, Singapore

P. Khuntontong · Z. Wang
Microfluidics Manufacturing Programme, Singapore Institute of Manufacturing Technology, A*STAR (Agency for Science, Technology and Research), 71 Nanyang Drive, Singapore 638075, Singapore

R. Soo
Cancer Science Institute of Singapore, Department of Haematology-Oncology, National University Hospital, 5 Lower Kent Ridge Rd, Singapore 119074, Singapore

et al. 2012; Denis et al. 2012; Tan et al. 2010). But the fact that CellSearch failed to detect CTCs in 36 % of metastatic breast cancer patients (Kasimir-Bauer et al. 2012) raises the concern: when a certain patient is deemed CTC-negative, is it due to the true CTC-negative status of the patient or a limitation of the technology? Thus, there is an urgent need to develop highly efficient and robust technologies for CTC isolation (Parkinson et al. 2012).

Different types of techniques have been employed to exploit the differences in morphological and physical properties between tumor cells and blood cells to isolate CTCs from blood samples. These include the bigger size of epithelial cells (Desitter et al. 2011; Lim et al. 2012; Xu et al. 2010; Lv et al. 2013), their difference in density (He et al. 2008), deformability (Tan et al. 2009) and dielectric properties (Gupta et al. 2012; Shim et al. 2013). In recent years, hydrodynamic sorting has also been employed to isolate CTCs from patients sample (Hur et al. 2011; Sun et al. 2013). Current technologies for CTC isolation have been well-reviewed (Arya et al. 2013; Chen et al. 2012; Zhe et al. 2011; Yu et al. 2011; Sun et al. 2011; Gerges et al. 2010; Hou et al. 2010). Epithelial Cell Adhesion Molecule (EpCAM) is a common surface marker for antibody based CTC isolation (Allard et al. 2004; Nagrath et al. 2007; Hoshino et al. 2011). CellSearch system employs the immunomagnetic EpCAM-positive selection for CTCs enrichment (Riethdorf et al. 2007). However, it has been noted that EpCAM-based method could significantly undercount the number of CTCs due to those cells that undergo Epithelial to Mesenchymal Transition (EMT) (Paterlini-Brechot and Benali 2007; Allard et al. 2004; Goeminne et al. 2000; Gorges et al. 2012). Size-based approaches, which are based on size and deformability of CTCs, are susceptible to the overlapping of size and density between the CTCs and white blood cells (WBCs) and the heterogeneity in size and deformability within the tumor cell subpopulations (Zhe et al. 2011; Park et al. 2012; Meng et al. 2004). It was recently reported that the tumor initiating sub-population of CTCs could easily pass through the obstacles that were designed to trap cancer cells (Alix-Panabières and Pantel 2013). Although it is fast, easy and relatively economical, the size-based CTC isolation technique suffers from an inherent recovery/purity trade-off. A negative depletion approach, which avoids labelling the cells or defining their size, has been recommended as an optimal approach (Yang et al. 2009).

A negative depletion approach depletes "normal" cells, including erythrocytes, leukocytes, platelets and leaves behind the "abnormal cells" such as CTCs for further analysis. In a typical negative enrichment approach, red blood cells (RBCs) are eliminated by chemical lysis or ficoll gradient centrifugation followed by depletion of WBCs. Then, the immunohistochemical staining or molecular analysis is applied to identify the "abnormal cells". Many currently developed negative depletion techniques involve multiple steps such as chemical RBC lysis and centrifugation that contribute to the risk of losing CTCs and adversely affect the cells of interest (Marrinucci et al. 2010; Park et al. 2012; Yang et al. 2009; Marrinucci et al. 2012; Cho et al. 2012; Tong et al. 2007; Lara et al. 2004). Chalmers et al. have demonstrated using such method with a CTC isolation efficiency of 83 % and 2.7 log10 enrichment (Yang et al. 2009; Lustberg et al. 2012). But this approach involves multiple sample processing steps, including RBC lysis (Yang et al. 2009), centrifugation, and multiple cell washing and re-suspension. It was reported in the previous works that RBC lysis and centrifugation steps can lead to 10 % and 30 % cell loss of spiked tumour cells respectively (Tong et al. 2007; Lara et al. 2004). Therefore, multiple sample processing steps are especially prone to compounding cell loss, which yields much less than 100 % overall CTC isolation efficiencies. A better implementation of a negative depletion approach that avoids multiple sample handling steps and usage of specialized instruments is needed.

In this paper, we introduce a microfluidic negative selection platform that combines a centrifugation-free WBC and chemical-free RBC depletion approach without manual sample transfer. In our approach, immunomagnetic WBC depletion is employed directly in 2 ml of whole blood. The WBC-depleted blood then flows through a microfluidic chip that contains a precision-manufactured micro slit membrane. The micro slit membrane is designed to selectively allow passage of RBCs and platelets while retaining as many nucleated cells. Thus, this method depletes WBCs and RBCs without the use of centrifugation or chemical lysis. In addition, it avoids multiple sample handling. By employing this simple and easy-to-use assay, more than 90 % WBC depletion and greater than 90 % recovery of CTCs in a relatively fast turnaround time of 1 h was achieved. In addition, since the sample is not subjected to any chemical manipulation, the exit volume can be used for complementary assays to extract molecular information such as serum protein or nucleic acid assays.

2 Materials and methods

2.1 Sample preparation

Blood was drawn from healthy donors of both genders into 6 ml BD Vacutainer K2 EDTA tubes (Becton Dickinson). Samples drawn had a cellular preservative (Ng et al. 2012; Truet et al. 2006) (Catlog#213358, Streck) manually added immediately after blood draw at a ratio of 1:1 and was maintained at 4 °C. The healthy donors had no known illness or fever at the time of draw and no history of malignant disease. Cancer patients' samples were obtained from National University Hospital under IRB approval. Similarly, the blood was drawn into 6 ml BD Vacutainer K2 EDTA tubes followed by the addition of cellular preservative as described above.

Samples drawn were maintained in a 4 °C environment from the point of collection to the place of processing and were processed within 48 h from the time of draw.

At the beginning of each experiment, 4 ml of preservative-added blood assay was pipetted from the Vacutainer tube into a 5 ml BD syringe barrel (Catlog#302135, USA). The mixture of 100 μl of customized anti-CD45 Tetrameric Antibody Complexes (TAC) (StemCell Technologies, Canada) and 100 μl of customized dextran-coated magnetic microparticles (StemCell Technologies Inc., Canada) was added to the sample and incubated for 30 min. The magnetic microparticles used here are 1 μm diameter in size. TAC are bi-specific and are able to recognize both dextran-coated magnetic beads and the target cell surface antigen (CD45) which is expressed on all human leukocytes. "The Big Easy" EasySep® Magnet was subsequently placed around the barrel to separate the labeled WBCs. Figure 1 shows the illustration of how magnetic particles bound to WBC through TAC. Afterwards, the WBC-depleted assay was put through a microfluidic chip that contains a micro slit membrane for target cell isolation. WBC depletion was determined by counting the cells before and after the immunomagnetic depletion procedure using an automated clinical haematology analyzer Horiba Micro ES60. (Horiba, Japan)

2.2 Micro slit membrane fabrication

A micro slit membrane was designed to deplete platelets, RBCs and smaller-sized leukocytes that escaped from immunomagnetic depletion, while retaining the majority of the other nucleated cells. The 10-μm thick micro slit membrane that was fabricated from Parylene-C. The membrane was circular in shape with a diameter of 13-mm and an active diameter of 9-mm. It consisted of periodically arranged precise slits with a slit dimension of 5.5-μm in width and 40-μm in length. This design was chosen after comparing it with other micro filter designs for cell separation due to its unique advantages in retaining CTCs (Ji et al. 2008; Zhu et al. 2007; Sajay et al. 2012; Sajay et al. 2013). Compared to commonly used circular/hexagonal microfilters openings, the rectangular slit design has the advantage of defraying the pressure applied across the cells trapped on membrane and preserving the viability and morphology of target cells (Xu et al. 2010). Moreover, this configuration resulted in a large fill factor of 44.5 %, which combined with upstream WBC depletion, allowed smooth blood flow of around 1 ml/min at very small air pressure of 3.5 mbar. The detailed fabrication process was reported previously (Sajay et al. 2013). Figure 2 shows the different views of the Parylene micro slit membrane.

2.3 Microfluidic chip

A precision-manufactured circular Parylene-C membrane was packaged in a microfluidic chip. Polymethyl methacrylate (PMMA) was used for substrate material because of its characteristics of good light transition and high chemical resistance. The chip is 25-mm wide and 75-mm long, which is the same size as the regular microscope slide. Additionally, it can be easily mounted on the stage of microscope for inspection. The chip consists of three layers in which the small geometries like channels are created by a precision micro milling technique. A polymer mesh was integrated 150 μm below the membrane as a support to prevent any potential deformation while the membrane was subjected to a positive pressure. Mesh size is 250×250 μm, which cells in sample can flow through. Different layers, membrane and mesh are integrated and laminated by thermal bonding technique.

Figure 3a shows a cross-section diagram of the circular membrane within the microfluidic chip. And, Fig. 3b shows the PMMA Microfluidic chip. The inlet of the chip was connected to a 5 ml syringe barrel for sample assay introduction. The 4 ml sample assay was delivered by a 1 mm wide connecting micro channel to the chamber of diameter 9 mm with the microslit filter membrane for target cell isolation. Subsequently, the waste from the outlet of the chip was collected in a 15 ml Falcon tube (Catlog#352097, BD). This

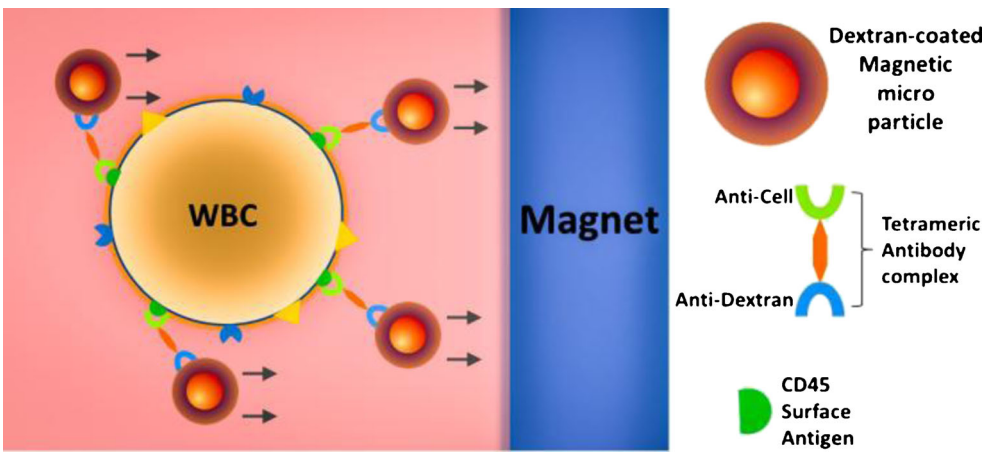

Fig. 1 Illustration of immunomagnetic WBC depletion in which magnetic particles bound to WBC through Tetrameric antibody complex in human whole blood

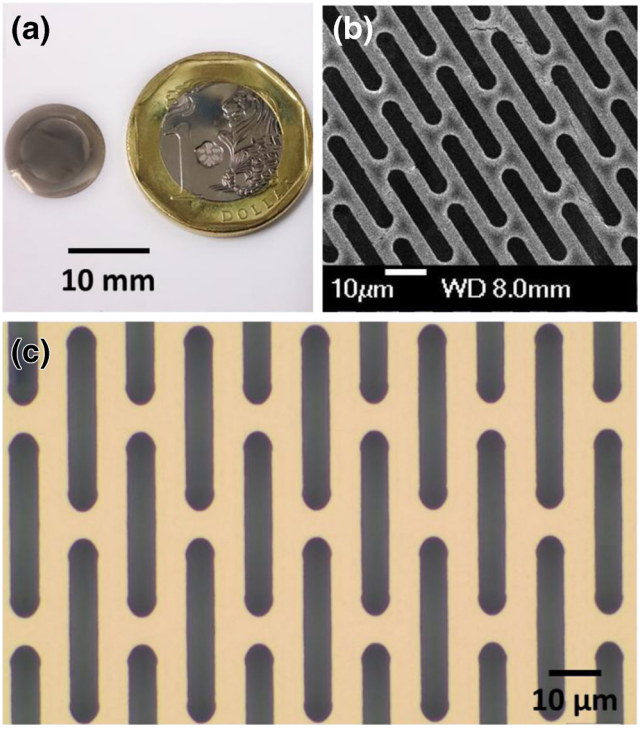

Fig. 2 Micro Slit membrane of diameter 13 mm containing slits with dimension 5.5×40 μm and a fill factor of 44.5 %. **a** An overview picture of the membrane **b** Image taken at 330× using scanning electron microscope (SEM) **c** Image taken at 50× using optical microscope

microfluidic chip provided an integrated and enclosed platform for sample manipulation, which avoided the risks of cell loss associated with sample transferring and handling.

2.4 Cell culture

Human lung cancer cell line NCI-H1975 and human breast cancer cell line MCF-7 were purchased from American Type Culture Collection (Manassas, VA). NCI-H1975 cells were cultured in RPMI 1640 (Catlog#22400-089, Invitrogen) supplemented with 10 % Fetal Bovine Serum (FBS) (Catlog#04-001-1A, Biological Industries). MCF-7 cells were cultured in DMEM (Catlog#11965-092, Invitrogen) supplemented with 10 % FBS. Cells were maintained at 37 °C in a humidified atmosphere containing 5 % CO_2 and harvested with trypsin before use. The cell suspensions were used only when their viability as assessed by Trypan blue exclusion exceeded 90 %.

2.5 Cell spiking

To demonstrate the sensitivity and linearity of the rare cell isolation assay, two sets of four 2 ml aliquots of peripheral blood diluted with 2 ml of cellular preservative were prepared. The first set (Set A) of four aliquots was spiked with a titration series of NCI-H1975 cells with approximately 10, 30, 50, or 100 cells per 2 ml blood. The second set (Set B) of four aliquots was spiked with a similar titration series as the first but with MCF-7 cells. For the reproducibility assay, two additional sets of replicates were prepared for Sets A and B. Cell spiking into blood was conducted before immunomagnetic WBC depletion step to fully mimic the process flow with patient blood.

Figure 4 shows the size distribution of cultured NCI-H1975 and MCF-7 cells. It is evident that the sizes of cells were ranging from 9 to 25 μm for NCI-H1975 cells. It is important to ensure that a good CTC isolation system is capable of capturing all nucleated cells with a wide range of cell sizes in order to achieve high isolation efficiency. Cells were not fixed prior to isolation in this work.

2.6 Staining protocol

To identify NCI-H1975 and MCF-7 cells on the precision micro-slit membranes, a mouse anti-pan Cytokeratin monoclonal antibody conjugated with fluorescein isothiocyanate (FITC) (Catlog#ab78478, Abcam) for cancer cells and a mouse anti-Human CD45 monoclonal antibody conjugated with Phycoerythrin(PE)-Dyomics 590 (Catlog#CLX48PE-DY590, Cedarlane Laboratories) for hematologic cells were used. After the microfiltration process, 500 μL of 4 % paraformaldehyde (PFA) (Catlog#P6148, Sigma) in 1× PBS was introduced to the chip and incubated for 15 min to fix the samples on the micro slit membrane. 1 ml of 1× PBS was then introduced to rehydrate the samples. The samples were then permeabilized with 0.25 % Triton X-100 (Catlog#X100, Sigma) in 1× PBS and incubated for 10 min. The samples were then washed with 1 ml of 1× PBS. After blocking non-specific binding sites with 5 % bovine serum albumin (BSA) (Catlog#A2153, Sigma) in 1× PBS for 30 min, the chip was incubated for 30 min with anti-pan Cytokeratin (FITC) and anti-Human CD45 (PE-Dyomics 590) antibodies in a dark

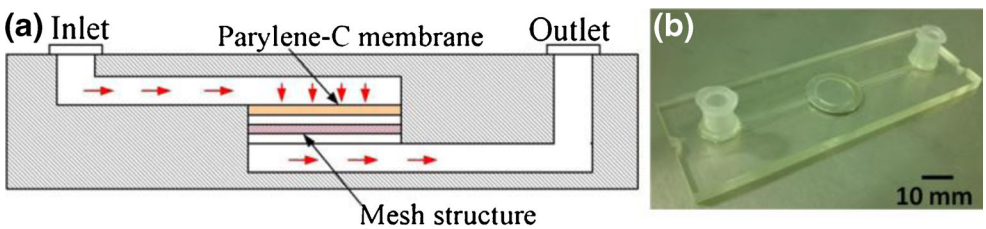

Fig. 3 Structures of microfluidic chip. **a** The cross-section of microfluidic chip. The sample assay was introduced from the inlet, through the membrane, and exited to the outlet. **b** The image of our microfluidic chip with luer connectors at the inlet and outlet

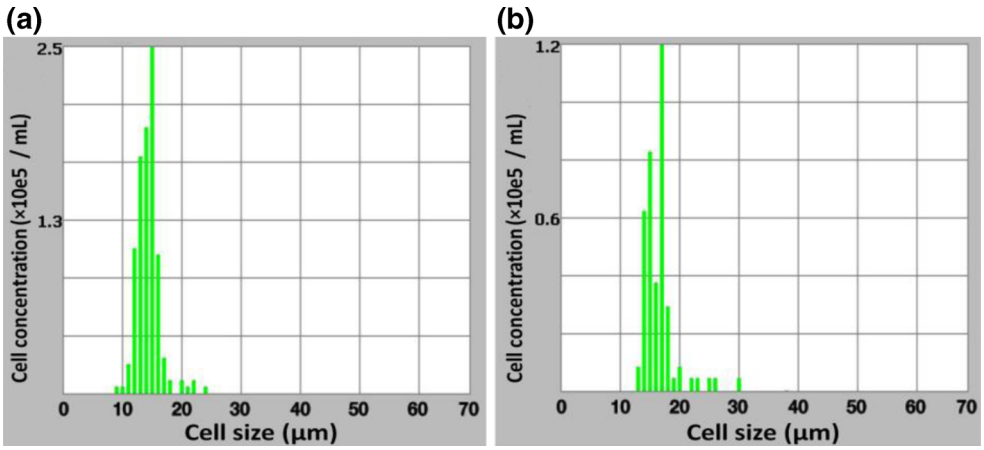

Fig. 4 Size distribution of cultured **a** NCI-H1975 lung cancer cell line **b** MCF-7 breast cancer cell line. Data obtained using an automated cell counter. (Luna, LogosBiosystems)

room. The samples were then washed with 1 ml of 1× PBS. After counter-staining with 1 µL of Hoechst 33342 (Catlog#H1399, Invitrogen) in 499 µL of 1× PBS, the samples were washed for the last time with 1 ml of 1× PBS to minimize background noise. Finally, the chip was mounted on an upright fluorescent microscope (BX61, Olympus) for CTC enumeration and sample analysis.

2.7 Experimental setup

The experimental setup and illustration of the microfluidic platform are shown in Fig. 5. The 5 ml syringe barrel containing blood sample conjugated with TAC and magnetic particle complex was placed within the magnet for immunomagnetic WBC depletion. This set up was placed directly above another 5 ml syringe barrel that was connected to the inlet of the microfluidic chip. Upon completion of the magnetic incubation period, the WBC-depleted blood was flowed through the chip setup under gravity. Subsequently, the WBC-depleted assay was driven by a constant 3.5-mBar air pressure (MV20 pump, Ibidi) through the microfluidic chip for microfiltration process. The applied pressure was monitored in real time by pump controller software.

The microfiltration process for 4 ml blood assay was completed in less than 5 min. 2 ml of 1× PBS was introduced and flowed continuously to wash and remove the remaining RBCs on the micro slit membrane. Fixation of cells followed by the staining protocol was initiated after the washing step. Chip was then removed from the connectors and inspected under a fluorescent microscope. The same 3.5 mBar air pressure was employed to deliver the reagents in all of the procedures, including washing, fixation, and staining steps.

2.8 Cell identification

Cell identification was conducted by fluorescence microscopy using an upright microscope (BX61, Olympus) with a motorized xy stage. Image capturing was performed by 14-bit monochrome ExiAqua fast 1394 CCD camera (QImaging, Canada). U-MWU2, U-MWIB2, and U-MSWG2 filter sets were used to visualize staining of Hoechst, FITC, and PE-Dyomics 590 probes. Motorized stage was controlled by a joystick to scan through the entire membrane. In addition, the software, Image Pro-Plus MDA (Media Cybernetics, USA), was employed to apply pseudo color to the acquired cell images. Cell counting and image capturing were performed using a 40× objective lens. The cell identification process was performed by an experienced molecular biologist specialized in cell pathology.

A CTC was defined as an object with the following criteria: (a) circular to oval morphology, (b) a visible nucleus (Hoechst positive), (c) negative staining for CD45, and (d) positive staining for Cytokeratin (Marrinucci et al. 2012; Tan et al. 2010). Results of cell enumeration are always expressed as the number of cells per 2 ml of blood.

2.9 Cell depletion and recovery

The depletion of WBCs by immunomagnetic method, cancer cell recovery and total WBC depletion on the membrane were determined as following:

$$WBC\ depletion(\%) = \frac{W_i - W_f}{W_i} \times 100$$

$$Recovery\ Efficiency(\%) = \frac{C_R}{C_S} \times 100$$

$$Total\ WBC\ Depletion\,(\log) = \log\frac{N_i}{N_f}$$

W_i is the total number of WBC in the original 2 ml sample and W_f is the number of WBC in sample after immunomagnetic WBC depletion. Both W_i and W_f were determined by an automated clinical haematology analyzer. C_S is the number of cancer cells spiked into the 4-ml blood assay prior to immunomagnetic WBC depletion process when C_R is the number of cancer cells isolated and counted on the micro

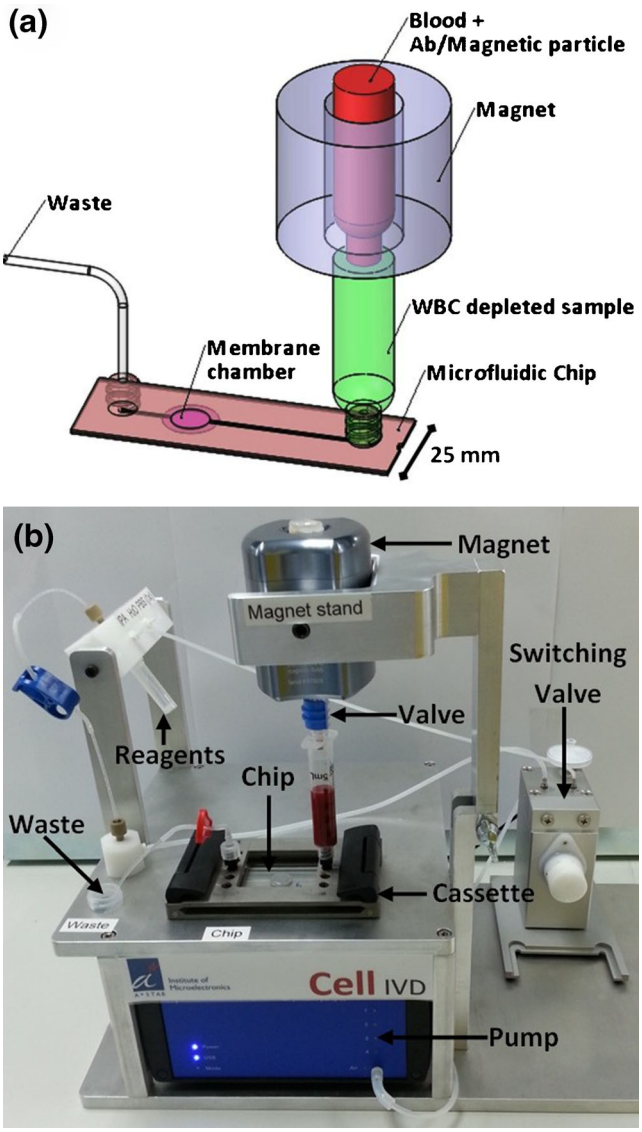

Fig. 5 Experimental setup for CTCs isolation from whole blood. **a** Schematic of main components in CTC isolation system and microfluidic chip setup. WBCs within the sample were depleted by immunomagnetic separation before flew down to chip to retain CTCs. **b** Photograph of the experimental setup of our CTC isolation system. Sample was driven by a pneumatic pressure regulated precisely by the pump

slit retention membrane through fluorescent microscopy. N_i is the total number of nucleated cells in the sample prior to the experiment, which is equal to W_i. And, N_f is the number of nucleated cells counted on the micro slit membrane by a Matlab-based automated image-processing algorithm, CellC (Selinummi et al. 2005). The WBC depletion is calculated by sampling after the immunomagnetic depletion step using an automated clinical haematology analyzer Horiba Micro ES60. Due to the limitation of the analyzer, for those samples with good depletion results, eg: remained WBCs is less than 0.1 M/ml, the WBC count is shown as 0 M/mL from the analyzer, which did not reflect the real number of remained WBC in the WBC-depleted assay. The total WBC depletion is a more realistic number, which is calculated by counting the number of physical WBC remained on the membrane.

3 Results and discussion

3.1 Upstream immunomagnetic WBC depletion

The numbers of WBCs in these experiments ranged between 4.5 and 11.6 million/ml. By employing our newly developed methodology, an average of 97 % of WBCs was depleted before reaching the micro slit membrane. Due to a high degree of WBC depletion before microfiltration, combined with a micro slit membrane with high fill factor, our microfluidic chip was able to process 4 ml assay in less than 5 min at a minimal positive pressure of 3.5-mbar, resulting in excellent morphology of retained cells. Figure 6 shows the upstream immunomagnetic WBC depletion data among 25 samples using Horiba Micro ES60.

3.2 On-chip cell counting and isolation efficiency

Negative controls were performed alongside experiments with spiked CTCs. Figure 7a shows the images taken under three different filters. Cells that were Hoechst-positive, CD45-negative and panCK-positive were considered as a CTC. No CTC cells were found in healthy donor blood samples. Next, various concentrations of cell lines were spiked in 2 ml of whole blood and processed through the cell isolation system. The isolated CTCs and other nucleated cells were retained on the micro slit membrane after the microfiltration process. The isolated target cells were fixed and stained according to our staining protocol for CTC identification and counting. Figure 7b and c show the images taken through three different

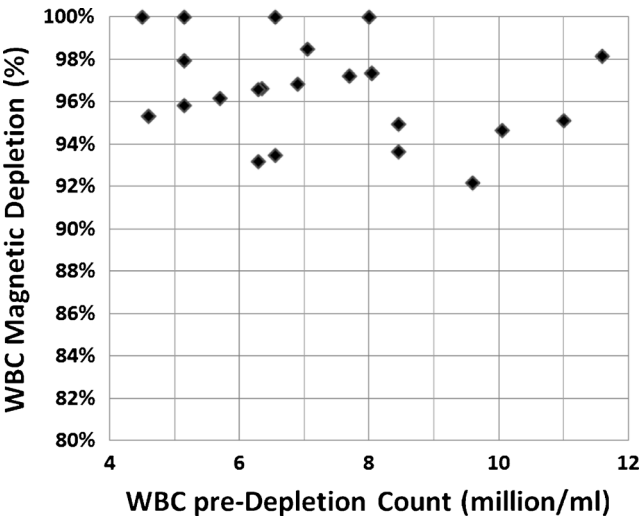

Fig. 6 Results of WBC depletion (in percentage) as a function of the concentration of WBCs in original blood (in million per millilitre) from 25 blood samples

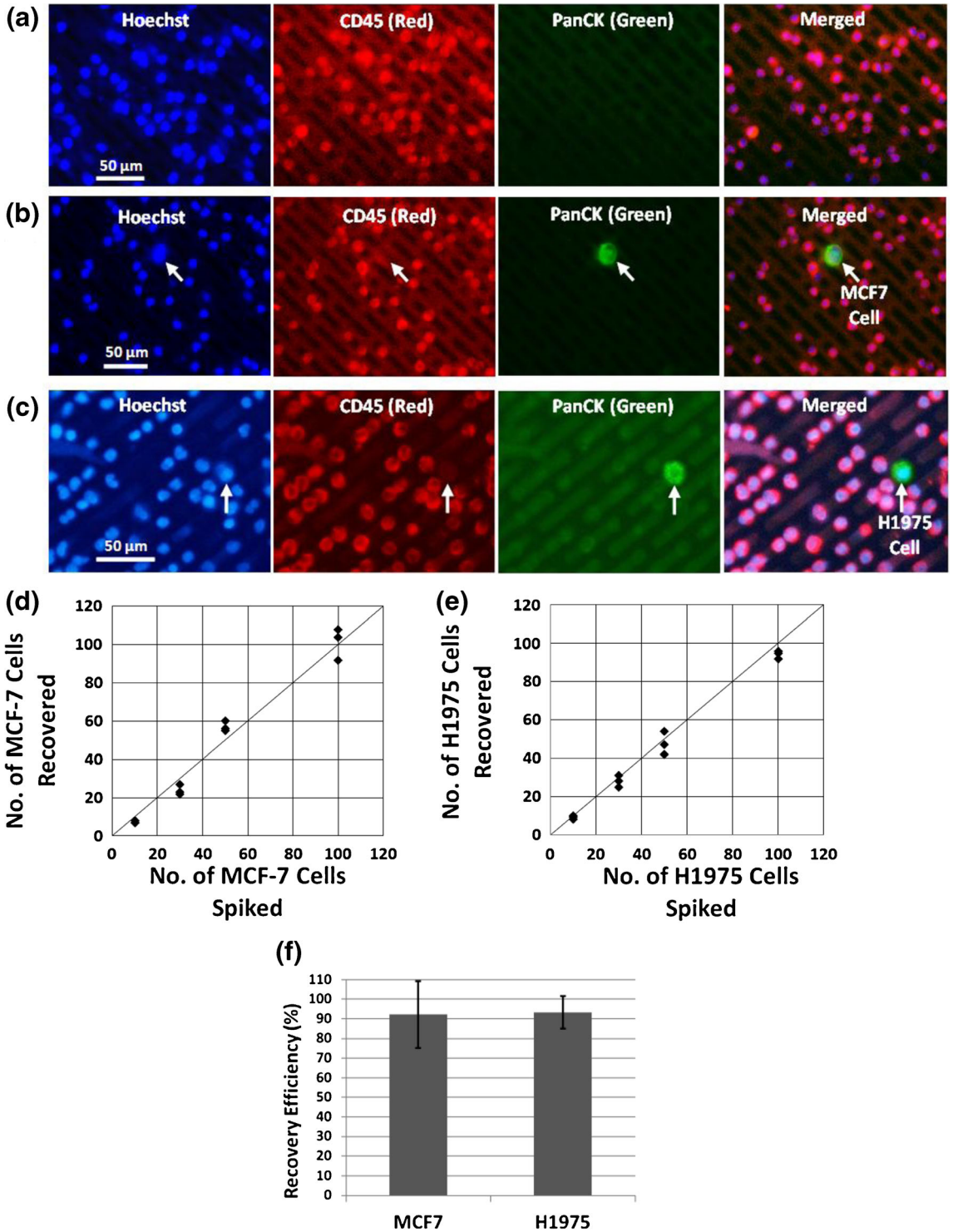

Fig. 7 Results of CTC isolation and enumeration. Images of cells captured on the micro slit membrane after processing healthy donor blood **a** Negative control, Blood without spiking any cancer cells. **b** blood that was spiked with MCF7 cells. **c** blood that was spiked with NCI-H1975 cells. The cell nucleus were stained with Hoechst (*blue*), the WBCs were stained by PE-labelled anti-CD45 (*red*) and the cancer cells were stained by FITC-labelled antibodies Pan-Cytokeratin (*green*). Cancer cells recovered from whole blood as a function of different spiking concentrations **d** MCF-7 **e** NCI-H1975 cancer cell lines. All experiments conducted with cells spiked for four spiking concentrations ($n=3$). **f** Chart showing the average recovery efficiency of MCF7 and NCI-H1975 cancer cells. The *error bars* represent standard deviations among all experiments

filters to indicate the CTC as Hoechst-positive, CD45-negative and pan-CK-positive. In addition, the merged images are also provided. Figure 7d and e show the number of CTCs, including MCF-7 and NCI-H1975, recovered and counted on

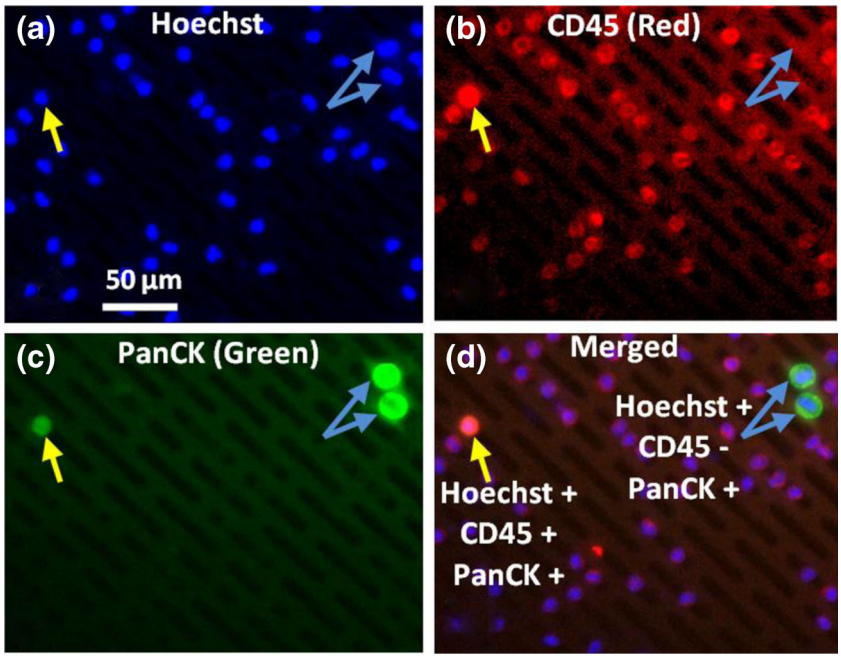

Fig. 8 Fluorescence image under different filters for cells identification and classification. **a** Hoechst stains cell nucleus. **b** PE-labelled anti-CD45 antibody stains CD45+ cells (WBCs). **c** FITC-labelled PanCK antibody stains PanCK+ cells (CTCs). **d** Merged image of (**a**) (**b**) and (**c**). The *blue arrows* indicate the cancer cells that are Hoechst-positive CD45-negtive and PanCK-positive when *yellow arrow* indicates the unknown artifact cell that is Hoechst-positive CD45-positive and PanCK-positive. Rest of the cells in the (**d**) is WBCs, which are Hoechst-positive CD45-positive and PanCK-negative

the micro slit membrane as a function of number of CTCs spiked into the 4 ml sample assay. An average of 92.17 % of MCF-7 were recovered across the spiking range of 10 to 100 cells ($n=3$ for each concentration). An average of 93.25 % of NCI-H1975 was recovered from using our system in the same spiking range of 10 to 100 cells. Figure 7f shows this data.

During our experiments, some cells were observed as double positive cells which expressed to both CD45 and pan-CK antibodies. We had very little knowledge about the origin and significance of these cells and therefore we excluded these from CTC enumeration (Lustberg et al. 2012; Stott et al. 2010). Figure 8 shows how cancer cells were distinguished from other cells.

3.3 On-chip purity

The number of WBCs was recorded before and after immunomagnetic depletion using an automated clinical haematology analyzer as discussed before. The final assay purity was determined by counting the number of nucleated cells retained on micro slit membrane alongside CTCs. Figure 9 shows the Hoechst-stained fluorescent image of nucleated cells captured by micro slit membrane from two experiments: one processed with immunomagnetic WBC-depleted blood sample with our protocol (Fig. 9a) and the other was without any WBC depletion steps (Fig. 9b). The latter took more than 30 min to finish the microfiltration process on our microfluidic chip. The images clearly demonstrate that the WBC-depleted sample has much lower number of nucleated cells on the membrane than one without depletion, which explains the smoother sample flow and higher purity of CTC enrichment by our system. RBCs were depleted >99.99 % and were barely found on the membrane surface. Automated imaging and image processing algorithms were employed to acquire high magnification images of Hoechst-stained cells on the membrane to determine the total number of nucleated cells on the membrane surface. Using this

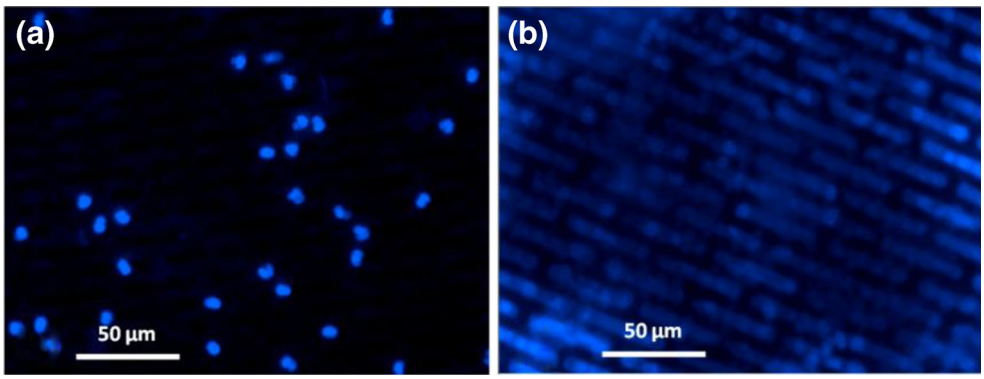

Fig. 9 Images showing nucleus of PBMCs captured on membrane. **a** Experiment was done with immunomagnetic WBCs depletion showing only few nucleated cells on the membrane. **b** Experiment was done without immunomagnetic WBCs depletion. Layers of WBCs were captured on the membrane which leads to a lower purity

Table 1 Cancer cell isolation and WBC depletion data by processing 2 ml of whole blood from 15 cancer patients

Patient	Cancer type	Pre count WBC (M/ml)[a]	Post count WBC (M/ml)[b]	Immuno-magnetic WBC depletion (%)	# of CTCs (per 2 ml)	Total WBC depletion[c]
1	NSCLC	6.55	0.00	100.00	22	2.76 log
2	NSCLC	8.00	0.00	100.00	15	2.79 log
3	NSCLC	11.60	0.22	98.15	1	2.46 log
4	NSCLC	11.00	0.54	95.11	12	2.61 log
5	NSCLC	10.05	0.54	94.63	11	2.03 log
6	NSCLC	4.50	0.00	100.00	19	2.35 log
7	NSCLC	8.65	0.22	97.46	2	2.50 log
8	NSCLC	5.90	0.00	100.00	1	2.75 log
9	NSCLC	11.00	0.22	98.00	3	2.22 log
10	NSCLC	16.40	0.43	97.38	51	2.45 log
11	NSCLC	5.45	0.22	95.96	7	2.01 log
12	NSCLC	9.85	0.54	94.52	2	2.13 log
13	CRC	9.60	0.75	92.16	11	2.40 log
14	CRC	3.90	0.11	97.18	20	2.03 log
15	CRC	8.30	0.65	92.17	13	2.18 log

[a] WBC count (million/ml) in original sample measured by using automated clinical hematology analyzer Horiba Micro ES60

[b] WBC count (million/ml) in sample after immunomagnetic depletion step measured by using automated clinical hematology analyzer Horiba Micro ES60. Due to the limitation of the analyzer, those samples which contain WBC less than 0.1 M/ml are shown as 0 M/ml

[c] Total WBC depletion was calculated by counting the number of physical WBC remained on the membrane after experiment by automated imaging and image processing

method, the average total nucleated cell depletion was determined to be 2.3 log10.

3.4 Clinical testing

To demonstrate the utility of our system in detecting CTCs from clinical patient samples, 15 clinical samples were received from National University Hospital, Singapore, to be processed on our system. These included 12 Non-Small-Cell Lung Carcinoma (NSCLC) and 3 colorectal (CRC) cancer case. These samples were processed through the CTC isolation and enumeration system. Our system successfully detected CTCs in 15 out of 15 patients based on the cell identification criteria of nucleus stain Hoechst-positive, CD45-negative

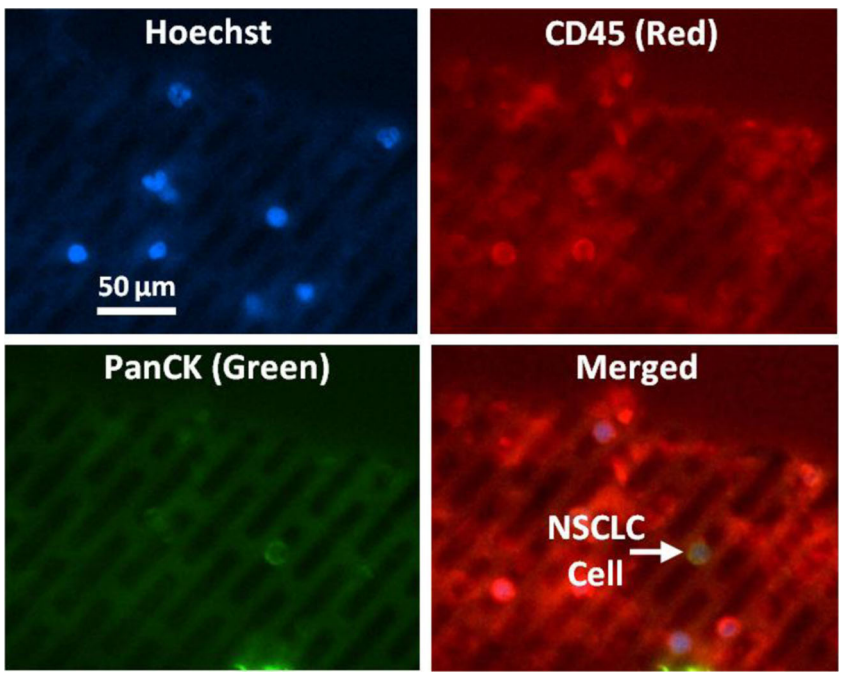

Fig. 10 CTC from a NSCLC patient sample was captured on the micro slit membrane and imaged under three different filters for fluorescent microscopy

and pan-CK-positive. Table 1 summarizes the results from the clinical testing. Figure 10 shows the images taken from one of NSCLC patient sample.

4 Conclusion

In the previous paper (Sajay et al. 2013), we tested our idea of negative enrichment by using upstream immunomagnetic WBC depletion and a micro-fabricated slit filter membrane retained by a commercial filter holder to isolate two GFP-tagged cell lines, which passed the initial test but was not fully representable for the real case. In addition, the membrane with isolated cells had to be transferred to microscope slide for inspection, which often resulted bad cell morphology and cell loss. In this paper, we completely demonstrated our simple, 2-step negative CTC enrichment protocol by using two non-GFP-tagged cells lines for spiking experiments and 15 clinical samples along with newly developed microfluidic chip and setup to perform full process of on-chip CTC isolation, staining and identification without any sample transferring. Our microfluidic chip platform showed a better sensitivity (10 vs 200 cells) compared to previous paper that used commercial holder to retain the microslit filter membrane fabricated in-house. Our method does not rely on either antigen expression, nor employs centrifugation and other extensive sample handling steps, which lead to compounded cell loss and are difficult to standardize. In our approach, an effective upstream immunomagnetic WBC depletion method was developed to deplete WBCs directly in whole blood. This was coupled with a downstream precision micro-slit membrane that performed a chemical-free and centrifugation-free RBC depletion as well as highly efficient CTC retention. This technique yields several benefits such as a) highly efficient, unbiased isolation of unfixed cells with excellent morphology, b) fast turnaround time, c) capable to accommodate larger amount of sample and can be scalable, d) amenable to full automation (hence standardization), and e) 2.3 log10 total WBC depletion which enables routine downstream molecular analysis. Although our slit membrane was designed to retain all nucleated cells, we observed that some cells did escape from capturing by our slit membrane. More cancer cell lines will be tested in order to better understand the capability of our slit membrane. Besides demonstrating high recovery from low spiked cell numbers, we also demonstrated 100 % CTC detection in 15 clinical patient samples. Further clinical studies are ongoing. Future version of the system will be fully automated for standardized implementation across multiple clinical sites. Efforts are underway to increase the total WBC depletion from 2.3 log to 4 log, while maintaining the current high recovery, which is potentially considered to be close to ideal for CTC isolation platforms.

Acknowledgments This work was supported by the Science and Engineering Research Council of A*STAR (Agency for Science, Technology and Research), Singapore under the grant number 1031490005. In addition, we greatly appreciate the support from Dr. Chaitanya Kantak for microslit membrane fabrication.

References

C. Alix-Panabières, K. Pantel, Circulating tumor cells: liquid biopsy of cancer. Clin. Chem. **59**, 110–118 (2013)

W.J. Allard, J. Matera, M.C. Miller, M. Repollet, M.C. Connelly, C. Rao, A.G. Tibbe, J.W. Uhr, L.W. Terstappen, Tumor cells circulate in the peripheral blood of all major carcinomas but not in healthy subjects or patients with nonmalignant diseases. Clin. Cancer Res. **10**(20), 6897–6904 (2004)

S.K. Arya, B. Lim, A.R. Abdur Rahman, Enrichment, detection and clinical significance of circulating tumor cell. Lab Chip **13**(11), 1995–2027 (2013)

G.T. Budd, Let me do more than count the ways: what circulating tumor cells can tell us about the biology of cancer. Mol. Pharm. **6**(5), 1307–1310 (2009)

J. Chen, J. Li, Y. Sun, Microfluidic approaches for cancer cell detection, characterization, and separation. Lab Chip **12**(10), 1753–1767 (2012)

E.H. Cho, M. Wendel, M. Luttgen, C. Yoshioka, D. Marrinucci, D. Lazar, E. Schram, J. Nieva, L. Bazhenova, A. Morgan, A.H. Ko, W.M. Korn, A. Kolatkar, K. Bethel, P. Kuhn, Characterization of circulating tumor cell aggregates identified in patients with epithelial tumors. Phys. Biol. **9**(1), 16001 (2012)

S. Denis, M. Keith, S. Kam, S. Alison, H. Richard, T. Don, J. Chunsheng, M. Aladin, T. David, D. Yi, C. Jason, W. Michele, P. Bill, C. Walter, A microfluidic system for the selection of circulating tumor cells that utilizes both affinity and size capture technologies. Cancer Res. **72**(8), 2389 (2012)

I. Desitter, B.S. Guerrouahen, N. Benali-Furet, J. Wechsler, P.A. Jänne, Y. Kuang, M. Yanagita, L. Wang, J.A. Berkowitz, R.J. Distel, Y.E. Cayre, A new device for rapid isolation by size and characterization of rare circulating tumor cells. Anticancer Res. **31**(2), 427–441 (2011)

N. Gerges, J. Rak, N. Jabado, New technologies for the detection of circulating tumour cells. Br. Med. Bull. **94**, 49–64 (2010)

J.C. Goeminne, T. Guillaume, M. Symann, Pitfalls in the detection of disseminated non-hematological tumor cells. Ann. Oncol. **11**(7), 785–792 (2000)

T.M. Gorges, I. Tinhofer, M. Drosch, L. Roese, T.M. Zollner, T. Krahn, O. Ahsen, Circulating tumour cells escape from EpCAM-based detection due to epithelial-to-mesenchymal transition. BMC Cancer **12**, 178 (2012)

V. Gupta, I. Jafferji, M. Garza, V.O. Melnikova, D.K. Hasegawa, R. Pethig, D.W. Davis, ApoStream(™), a new dielectrophoretic device for antibody independent isolation and recovery of viable cancer cells from blood. Biomicrofluidics **6**(2), 024133 (2012)

W. He, S.H. Kularatne, K.R. Kalli, F.G. Prendergast, R.J. Amato, G.G. Klee, L.C. Hartmann, P.S. Low, Quantitation of circulating tumor cells in blood samples from ovarian and prostate cancer patients using tumor-specific fluorescent ligands. Int. J. Cancer **123**(8), 1968–1973 (2008)

K. Hoshino, Y.Y. Huang, N. Lane, M. Huebschman, J.W. Uhr, E.P. Frenkel, X. Zhang, Microchip-based immunomagnetic detection of circulating tumor cells. Lab Chip **11**(20), 3449–3457 (2011)

J. Hou, K. Matthew, W. Tim, M. Karen, S. Robert, B. Fiona, D. Caroline, Circulating tumor cells, enumeration and beyond. Cancers **2**, 1236–1250 (2010)

S.C. Hur, A.J. Mach, D. Di Carlo, High-throughput size-based rare cell enrichment using microscale vortices. Biomicrofluidics **5**(2), 022206 (2011)

H.M. Ji, V. Samper, Y. Chen, C.K. Heng, T.M. Lim, L. Yobas, Silicon-based microfilters for whole blood cell separation. Biomed. Microdevices **10**(2), 251–257 (2008)

H.J. Kahn, A. Presta, L.Y. Yang, J. Blondal, M. Trudeau, L. Lickley, C. Holloway, D.R. McCready, D. Maclean, A. Marks, Enumeration of circulating tumor cells in the blood of breast cancer patients after filtration enrichment: correlation with disease stage. Breast Cancer Res. Treat. **86**(3), 237–247 (2004)

S. Kasimir-Bauer, O. Hoffmann, D. Wallwiener, R. Kimmig, T. Fehm, Expression of stem cell and epithelial–mesenchymal transition markers in primary breast cancer patients with circulating tumor cells. Breast Cancer Res. **14**(1), 15 (2012)

O. Lara, X. Tong, M. Zborowski, J.J. Chalmers, Enrichment of rare cancer cells through depletion of normal cells using density and flow-through, immunomagnetic cell separation. Exp. Hematol. **2**(10), 891–904 (2004)

L.S. Lim, M. Hu, M.C. Huang, W.C. Cheong, A.T. Gan, X.L. Looi, S.M. Leong, E.S. Koay, M.H. Li, Microsieve lab-chip device for rapid enumeration and fluorescence *in situ* hybridization of circulating tumor cells. Lab Chip **12**(21), 4388–4396 (2012)

M. Lustberg, K.R. Jatana, M. Zborowski, J.J. Chalmers, Emerging technologies for CTC detection based on depletion of normal cells. Recent Results Cancer Res. **195**, 97–110 (2012)

P. Lv, Z. Tang, X. Liang, M. Guo, R.P.S. Han, Spatially gradated segregation and recovery of circulating tumor cells from peripheral blood of cancer patients. Biomicrofluidics **7**, 034109 (2013)

D. Marrinucci, K. Bethel, D. Lazar, J. Fisher, E. Huynh, P. Clark, R. Bruce, J. Nieva, P. Kuhn, Cytomorphology of circulating colorectal tumor cells: a small case series. J. Oncol. (2010). doi:10.1155/2010/861341

D. Marrinucci, K. Bethel, A. Kolatkar, M.S. Luttgen, M. Malchiodi, F. Baehring, K. Voigt, D. Lazar, J. Nieva, L. Bazhenova, A.H. Ko, W.M. Korn, E. Schram, M. Coward, X. Yang, T. Metzner, R. Lamy, M. Honnatti, C. Yoshioka, J. Kunken, Y. Petrova, D. Sok, D. Nelson, P. Kuhn, Fluid biopsy in patients with metastatic prostate, pancreatic and breast cancers. Phys. Biol. **9**(1), 016003 (2012)

S. Meng, D. Tripathy, E.P. Frenkel, S. Shete, E.Z. Naftalis, J.F. Huth, P.D. Beitsch, M. Leitch, S. Hoover, D. Euhus, B. Haley, L. Morrison, T.P. Fleming, D. Herlyn, L.W. Terstappen, T. Fehm, T.F. Tucker, N. Lane, J. Wang, J.W. Uhr, Circulating tumor cells in patients with breast cancer dormancy. Clin. Cancer Res. **10**, 8152–8162 (2004)

S. Nagrath, L.V. Sequist, S. Maheswaran, D.W. Bell, D. Irimia, L. Ulkus, M.R. Smith, E.L. Kwak, S. Digumarthy, A. Muzikansky, P. Ryan, U.J. Balis, R.G. Tompkins, D.A. Haber, M. Toner, Isolation of rare circulating tumour cells in cancer patients by microchip technology. Nature **450**, 1235–1239 (2007)

A.A. Ng, B.T. Lee, T.S. Teo, M. Poidinger, J.E. Connoll, Optimal cellular preservation for high dimensional flow cytometric analysis of multicentre trials. J. Immunol. Methods **385**, 79–89 (2012)

J.M. Park, J.Y. Lee, J.G. Lee, H. Jeong, J.M. Oh, Y.J. Kim, D. Park, M.S. Kim, H.J. Lee, J.H. Oh, S.S. Lee, W.Y. Lee, N. Huh, Highly efficient assay of circulating tumor cells by selective sedimentation with a density gradient medium and microfiltration from whole blood. Anal. Chem. **84**(17), 7400–7407 (2012)

D.R. Parkinson, N. Dracopoli, B. Gumbs Petty, C. Compton, M. Cristofanilli, A. Deisseroth, D.F. Hayes, G. Kapke, P. Kumar, J.S. Lee, M.C. Liu, R. McCormack, S. Mikulski, L. Nagahara, K. Pantel, S. Pearson-White, E.A. Punnoose, L.T. Roadcap, A.E. Schade, H.I. Scher, C.C. Sigman, G.J. Kelloff, Considerations in the development of circulating tumor cell technology for clinical use. J. Transl. Med. **10**, 138 (2012)

P. Paterlini-Brechot, N.L. Benali, Circulating tumor cells (CTC) detection: clinical impact and future directions. Cancer Lett. **253**(2), 180–204 (2007)

E. Racila, D. Euhus, A.J. Weiss, C. Rao, J. McConnell, L.W. Terstappen, J.W. Uhr, Detection and characterization of carcinoma cells in the blood. Proc. Natl. Acad. Sci. U. S. A. **95**(8), 4589–4594 (1998)

S. Riethdorf, K. Pantel, Disseminated tumor cells in bone marrow and circulating tumor cells in blood of breast cancer patients: current state of detection and characterization. Pathobiology **75**(2), 140–148 (2008)

S. Riethdorf, H. Fritsche, V. Müller, T. Rau, C. Schindlbeck, B. Rack, W. Janni, C. Coith, K. Beck, F. Janicke, S. Jackson, T. Gornet, M. Cristofanilli, K. Pantel, Detection of circulating tumor cells in peripheral blood of patients with metastatic breast cancer: a validation study of the Cell Search system. Clin. Cancer Res. **13**(3), 920–928 (2007)

R. Rolle, U. Günzel, B. Pachmann, K. Willen, K. Höffken, Pachmann, Increase in number of circulating disseminated epithelial cells after surgery for non-small cell lung cancer monitored by MAINTRA C(R) is a predictor for relapse: a preliminary report. World J. Surg. Oncol. **3**(1), 18 (2005)

B.G. Sajay, L. Yuxin, C. Chia-Pin, P.D. Puiu, A.R.A. Rahman, Optimization of breast tumor cells isolation efficiency and purity by membrane filtration. World Acad. Sci. Eng. Technol. **69**, 801–804 (2012)

B.G. Sajay, C.P. Chang, H. Ahmad, W.C. Chung, P.D. Puiu, A.R. Rahman, Towards an optimal and unbiased approach for tumor cell isolation. Biomed. Microdevices **15**(4), 699–709 (2013)

J. Selinummi, J. Seppala, O. Yli-Harja, J.A. Puhakka, Software for quantification of labeled bacteria from digital microscope images by automated image analysis. Biotechniques **39**(6), 859–863 (2005)

S. Shim, K. Stemke-Hale, A.M. Tsimberidou, J. Noshari, T.E. Anderson, P.R. Gascoyne, Antibody-independent isolation of circulating tumor cells by continuous-flow dielectrophoresis. Biomicrofluidics **7**(1), 011807 (2013)

S.L. Stott, C.H. Hsu, D.I. Tsukrov, M. Yu, D.T. Miyamoto, B.A. Waltman, S.M. Rothenberg, A.M. Shah, M.E. Smas, G.K. Korir, F.P. Floyd, A.J. Gilman, J.B. Lord, D. Winokur, S. Springer, D. Irimia, S. Nagrath, L.V. Sequist, R.J. Lee, K.J. Isselbacher, S. Maheswaran, D.A. Haber, M. Toner, Isolation of circulating tumor cells using a microvortex-generating herringbone-chip. Proc. Natl. Acad. Sci. U. S. A. **107**, 18392–18397 (2010)

Y.F. Sun, X.R. Yang, J. Zhou, S.J. Qiu, J. Fan, Y. Xu, Circulating tumor cells: advances in detection methods, biological issues, and clinical relevance. J. Cancer Res. Clin. Oncol. **137**(8), 1151–1173 (2011)

J. Sun, C. Liu, M. Li, J. Wang, Y. Xianyu, G. Hu, X. Jiang, Size-based hydrodynamic rare tumor cell separation in curved microfluidic channels. Biomicrofluidics **7**(1), 011802 (2013)

S.J. Tan, L. Yobas, G.Y. Lee, C.N. Ong, C.T. Lim, Microdevice for the isolation and enumeration of cancer cells from blood. Biomed. Microdevices **11**(4), 883–892 (2009)

S.J. Tan, R.L. Lakshmi, P. Chen, W.T. Lim, L. Yobas, C.T. Lim, Versatile label free biochip for the detection of circulating tumor cells from peripheral blood in cancer patients. Biosens. Bioelectron. **26**(4), 1701–1705 (2010)

X. Tong, L. Yang, J.C. Lang, M. Zborowski, J. Chalmers, Application of immunomagnetic cell enrichment in combination with RT-PCR for the detection of rare circulating head and neck tumor cells in human peripheral blood. Cytometry B Clin. Cytom. **72**(5), 310–323 (2007)

A.A. Truet, A. Letizia, E. Malyangu, F. Sinyangwe, B.N. Morales, N.F. Crum, S.M. Crowe, Efficacy of Cyto-Chex blood preservative for delayed manual CD4 testing using Dynal T4 Quant CD4 test among HIV-infected persons in Zambia. J. Acquir. Immune Defic. Syndr. **41**(2), 168–174 (2006)

T. Xu, B. Lu, Y.C. Tai, A. Goldkorn, A cancer detection platform which measures telomerase activity from live circulating tumor cells captured on a microfilter. Cancer Res. **70**(16), 6420–6426 (2010)

L. Yang, J.C. Lang, P. Balasubramanian, K.R. Jatana, D. Schuller, A. Agrawal, M. Zborowski, J.J. Chalmers, Optimization of an enrichment process for circulating tumor cells from the blood of head and neck cancer patients through depletion of normal cells. Biotechnol. Bioeng. **102**(2), 521–534 (2009)

M. Yu, S. Stott, M. Toner, S. Maheswaran, D.A. Haber, Circulating tumor cells: approaches to isolation and characterization. J. Cell Biol. **192**(3), 373–382 (2011)

X. Zhe, M.L. Cher, R.D. Bonfil, Circulating tumor cells: finding the needle in the haystack. Am. J. Cancer Res. **1**(6), 740–751 (2011)

L. Zhu, X.L. Peh, H.M. Ji, C.Y. Teo, H.H. Feng, W.T. Liu, Cell loss in integrated microfluidic device. Biomed. Microdevices **9**(5), 745–750 (2007)

V. Zieglschmid, C. Hollmann, O. Böcher, Detection of disseminated tumor cells in peripheral blood. Crit. Rev. Clin. Lab. Sci. **42**(2), 155–196 (2005)